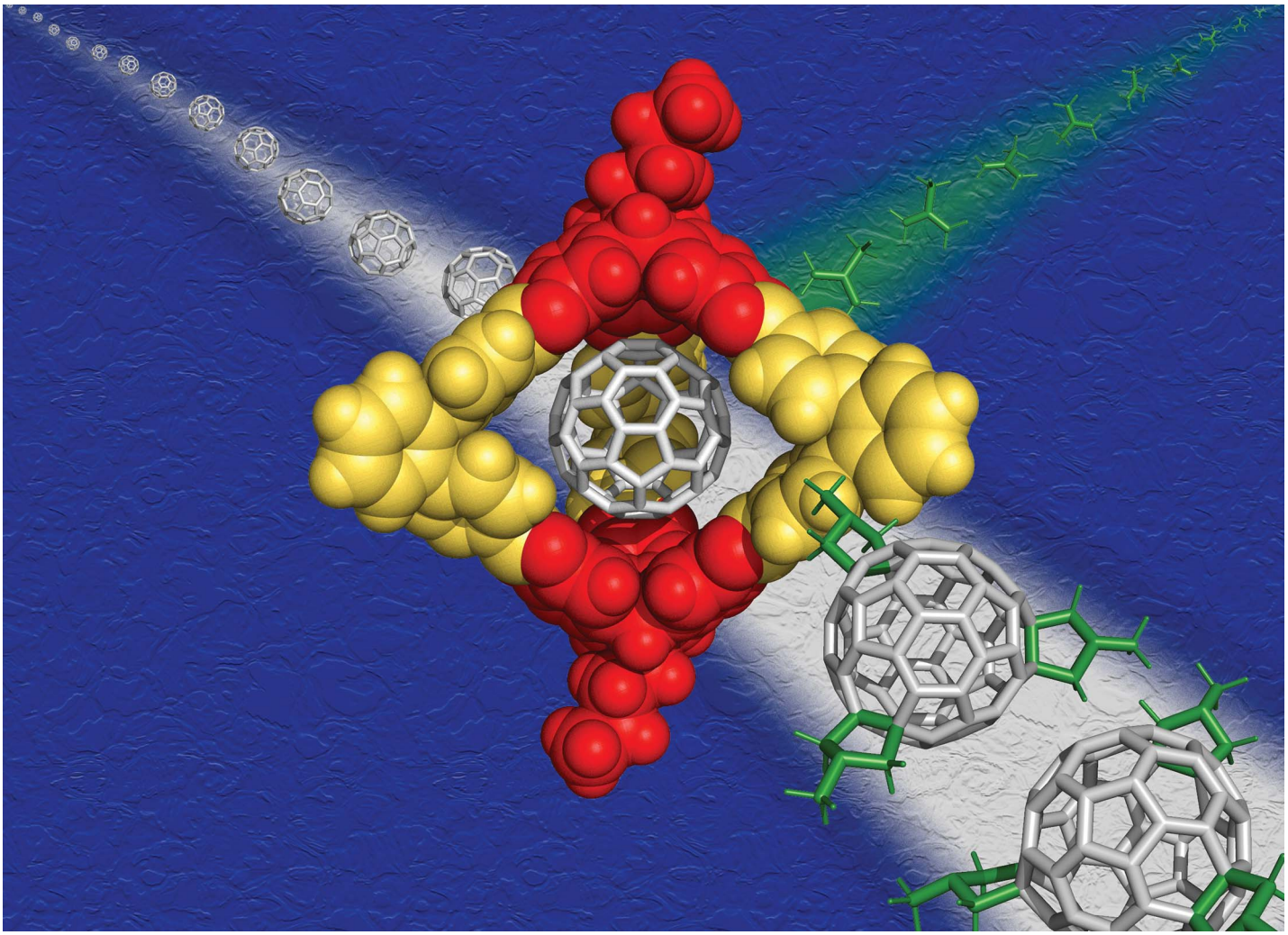

Showcasing research from PD Dr. Florian Beuerle's laboratory, Institut für Organische Chemie, Julius-Maximilians-Universität Würzburg, Germany.

A covalent organic cage compound acting as a supramolecular shadow mask for the regioselective functionalization of C_{60}

A trigonal-bipyramidal covalent organic cage compound readily forms highly stable 1:1 complexes with fullerenes C_{60} and C_{70}. These capsules serve as nano-sized shadow masks to guide the exohedral functionalization of encapsulated C_{60}. Prato reactions are limited to threefold addition and the preferred *trans*-3, *trans*-3, *trans*-3 addition pattern perfectly matches the symmetry and spatial arrangement of the three cage windows.

As featured in:

See Florian Beuerle *et al.*, *Chem. Sci.*, 2020, **11**, 8409.

ROYAL SOCIETY OF CHEMISTRY

rsc.li/chemical-science

Registered charity number: 207890

Chemical Science

ROYAL SOCIETY OF CHEMISTRY

EDGE ARTICLE

View Article Online
View Journal | View Issue

Check for updates

Cite this: *Chem. Sci.*, 2020, **11**, 8409

All publication charges for this article have been paid for by the Royal Society of Chemistry

Received 4th June 2020
Accepted 6th July 2020

DOI: 10.1039/d0sc03131c

rsc.li/chemical-science

A covalent organic cage compound acting as a supramolecular shadow mask for the regioselective functionalization of C_{60}†‡

Viktoria Leonhardt,[ab] Stefanie Fimmel,[b] Ana-Maria Krause[ab] and Florian Beuerle *[ab]

A trigonal-bipyramidal covalent organic cage compound serves as an efficient host to form stable 1 : 1-complexes with C_{60} and C_{70}. Fullerene encapsulation has been comprehensively studied by NMR and UV/Vis spectroscopy, mass spectrometry as well as single-crystal X-ray diffraction. Exohedral functionalization of encapsulated C_{60} *via* threefold Prato reaction revealed high selectivity for the symmetry-matched all-*trans*-3 addition pattern.

Introduction

Fullerenes act as spherically arranged electron-deficient polyolefins.[1] Their unique electronic structures facilitate potential applications in medicine,[2] photovoltaics[3] and organic electronics.[4] Synthetically, addition reactions, *e.g.*, Diels–Alder,[5] Bingel,[6] and Prato[7] reactions or other dipolar cycloadditions,[8] exploit the inherent strain energy of the curved double bonds, thus leading to a multitude of exohedrally functionalized derivatives.[9] I_h symmetrical C_{60} as the most abundant fullerene gives only one monoadduct. However, the number of potential regioisomers quickly raises to 8 (ref. 9*d*) and 46 (ref. 9*a* and *e*) for bis and trisaddition, respectively. The precise spatial organization of the individual addends identifies such multiple adducts as highly promising building blocks for 3D molecular architectures, *e.g.*, dendritic systems[10] or extended metal–organic[11] and supramolecular[12] frameworks. However, regioselectivity is generally governed by a combination of statistical and kinetic factors.[13] Thereby, the second addition step usually serves as a bottle neck for the selective formation of higher adducts and individual regioisomers have to be purified, if at all possible, by tedious HPLC chromatography. In some cases, specific addition patterns such as $C_{60}Cl_6$,[14] $C_{60}Ph_5H$,[15] or octahedral hexakisaddition[9c,16] have been obtained in surprisingly high purity under thermodynamic control.

Following a tether-directed remote functionalization approach that was introduced by the Diederich group,[17] all seven sterically possible bisadducts for methanofullerenes have been obtained by means of a covalent fixation of the two reactive sites in suitable tether systems.[9a] For higher adducts however, only a few tethers for privileged addition patterns are so far available.[18] Elaborate tether synthesis and limitations in post-synthetic modification further hamper this approach. In contrast, any supramolecular prealignment of the reactants or an *in situ* activation of specific double bonds is much more tempting. Seminal work by Guldi, Torres and coworkers on Prato reactions for a phthalocyanine aldehyde showed the highly selective formation of *cis*-1 bisadducts mediated by π–π interactions between the chromophores.[19] More recently, von Delius and coworkers reported the preferred formation of *trans*-bisadducts for Bingel reactions on C_{60}⊂[10]cyclo-paraphenylene.[20] When applying more sophisticated cage structures with a spatially precise orientation of multiple pore windows as hosts, the regioselective formation of higher adducts appears feasible (Fig. 1).

In recent years, a large variety of organic and metallosupramolecular cage receptors for fullerenes have been reported.[21] Selective binding was utilized for the separation of fullerene mixtures[22] and electron transfer was studied for dye-attached complexes.[23] Nitschke and coworkers reported on the selective encapsulation of Diels–Alder bisadduct mixtures within the cavity of an $Fe^{II}_8L_6$ cage. However, the regioselectivity for the encapsulation has not been investigated.[24] The Clever group used a bowl-shaped $[Pd^{II}_2L_3(MeCN)_2]^{4+}$ cage as a supramolecular protecting group for the selective monofunctionalization of encapsulated C_{60}.[25] The square-planar arrangement of the four cage windows for a metallosupramolecular fullerene sponge was recently utilized for the exclusive formation of all-*e* Bingel tetrakisadducts of C_{60}, even

[a]*Universität Würzburg, Institut für Organische Chemie, Am Hubland, 97074 Würzburg, Germany. E-mail: florian.beuerle@uni-wuerzburg.de*

[b]*Universität Würzburg, Center for Nanosystems Chemistry (CNC), Bavarian Polymer Institute (BPI), Theodor-Boveri-Weg, 97074 Würzburg, Germany*

† Electronic supplementary information (ESI) available. CCDC 1913637. For ESI and crystallographic data in CIF or other electronic format see DOI: 10.1039/d0sc03131c

‡ C_{60}⊂**1**: $C_{60}⊂C_{106}H_{72}B_6O_4·(C_7H_{11}BrO_4)_2$, M = 2801.23 g mol^{-1}, monoclinic, $C2/c$, a = 23.3258(10), b = 22.5169(10), c = 31.3889(10) Å, α = 90, β = 91.177(2), γ = 90°, V = 16 482.7(12) Å^3, Z = 4, $\rho_{calc.}$ = 1.129 g cm^{-3}, $\mu_{(CuK\alpha)}$ = 1.129 mm^{-1}, T = 100(2) K; 168 505 independent measured reflections. F^2 refinement, R_1 = 0.1264, wR_2 = 0.4437 (observed), 16 220 independent observed reflections (R_{int} = 0.0337) [$|F_o| > 4\sigma(|F_o|)$], $2\Theta \leq 144.72°$], 1100 parameters, 490 restraints.

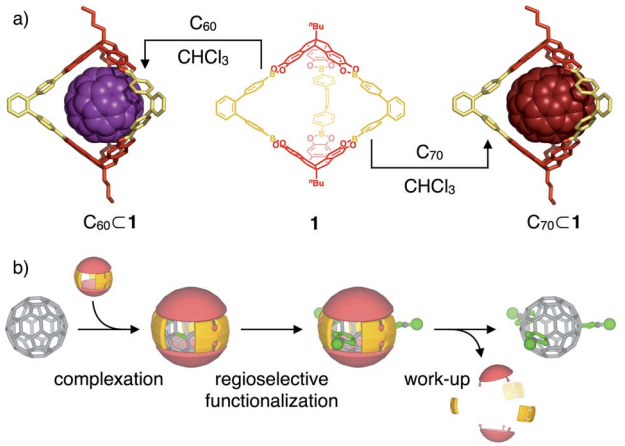

Fig. 1 (a) Supramolecular complexation of fullerenes C_{60} and C_{70} within the cavity of covalent organic boronate ester cage **1** (molecular structures of inclusion complexes are derived from semiempirical PM6 modeling); (b) schematical representation for the use of C_{60}-cage complexes as shadow masks for a regioselective exohedral C_{60} functionalization.

under catalytic conditions.[26] This masking strategy provides a significant improvement over the multistep orthogonal transposition approach[27] as the so far only practicable synthetic route for this addition pattern. Despite these initial examples, no cage templates to control the inherently less selective Prato reaction have been reported so far.

Results and discussion

Recently, we utilized the unique orthogonal arrangement of the three aromatic wings in C_{3v} symmetrical hexahydroxy tribenzotriquinacenes (TBTQs)[28] for the design and synthesis of covalent organic cage compounds[21f,29] *via* dynamic covalent boronate ester formation. By varying the bite angle of the diboronic acid counterpart, a series of cages[30] with trigonal-bipyramidal, tetrahedral or cubic shape and sizes ranging from 1.9 to 3.5 nm (solvodynamic diameters derived from DOSY NMR) were obtained. As fullerene binding was already shown for some π-extended TBTQ derivatives,[31] we tested the host properties of these cages. After saturation with either C_{60} or C_{70} by standing over pristine fullerenes for 24 hours at room temperature, fullerene uptake was analysed by UV/Vis absorption spectroscopy. No additional absorption in the range of 350 to 600 nm, which would indicate fullerene complexation, was observed for $CHCl_3$ solutions of a methoxy-protected TBTQ precursor and a large cubic cage (Fig. S5 and S6†). In case of trigonal-bipyramidal [2 + 3] cage **1** however, a linear correlation between the host concentration and additional absorption features characteristic for C_{60} and C_{70}, respectively, clearly indicated uptake of both fullerenes (Fig. S7†).

Further evidence for encapsulation was obtained by MALDI-TOF MS. The isotope patterns for the major signals at m/z = 2323.57 and 2442.67 are in excellent agreement with the respective 1 : 1 host–guest complexes $C_{60}\subset$**1** and $C_{70}\subset$**1** (Fig. 1). Remarkably, no signals for the empty cages besides small peaks for pristine C_{60} or C_{70} are detected for 1 : 1 mixtures (Fig. 2a and b). Semiempirical molecular modeling on the PM6 level revealed that the two TBTQ units in **1** are indeed perfectly preorganized for efficient encapsulation of one fullerene molecule. The distance of the two TBTQ *closo*-atoms in **1**, $C_{60}\subset$**1** and $C_{70}\subset$**1** only slightly changes from 1.55 to 1.66 and 1.69 nm (Fig. S1†). In the case of the larger cubic assemblies, only empty cages and no complexes were detected in MALDI measurements (Fig. S10†). Here, the increased distance between two TBTQs does not allow any favourable interaction of one fullerene with two TBTQs, thus preventing complexation.

For a quantitative analysis, $CHCl_3$ solutions of fullerenes C_{60} and C_{70} were titrated with a stock solution of **1** and absorption changes were plotted against cage concentration (see ESI† for details). Global fitting to a 1 : 1 binding model revealed complexation constants of $6.3 \pm 0.4 \times 10^5$ M^{-1} and $5.3 \pm 0.4 \times 10^5$ M^{-1} for C_{60} and C_{70}, respectively (Fig. 2c and d). Apparently, there is no significant preference for either C_{60} or C_{70}, which is presumably attributed to opposing effects of better size and shape matching for C_{60} and larger dispersion interactions for C_{70}.

Ultimately, single crystals suitable for X-ray diffraction were obtained during reactivity studies (see below) for the C_{60} complex. $C_{60}\subset$**1** crystallizes in the monoclinic space group *C*2/*c*.† Fig. 3b shows an ORTEP representation of the 1 : 1 inclusion complex. Whereas the host could be nicely refined, much higher disorder was observed for the guest indicating a very low barrier for internal C_{60} rotation.

Specific shifting of cage protons in ^{1}H NMR spectra of **1** in $CDCl_3$ in the presence of 3 equivalents of solid C_{60} revealed instantaneous complex formation (Fig. 3a). The rather small shifts might be explained by the assumption that spherical C_{60} is freely rotating within the cavities and the fact, that the para

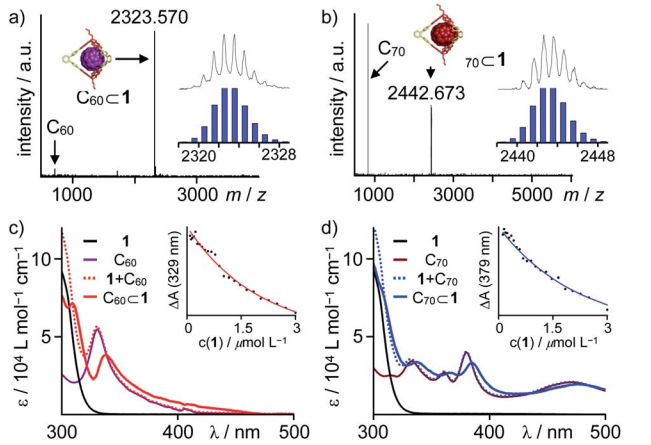

Fig. 2 MALDI-TOF MS (TCNQ, $CHCl_3$) for 1 : 1 mixtures of **1** and (a) C_{60} and (b) C_{70} (insets show comparison of measured and simulated isotope patterns); UV/Vis titration experiments for complex formation between **1** and (c) C_{60} (black **1**, purple C_{60}, dotted red **1** + C_{60}, red $C_{60}\subset$**1** derived from global fit to 1 : 1 model, inset shows fit to 1 : 1 model at λ = 329 nm) and (d) C_{70} (black **1**, brown C_{70}, dotted blue **1** + C_{70}, blue $C_{70}\subset$**1** derived from global fit to 1 : 1 model, inset shows fit to 1 : 1 model at λ = 379 nm).

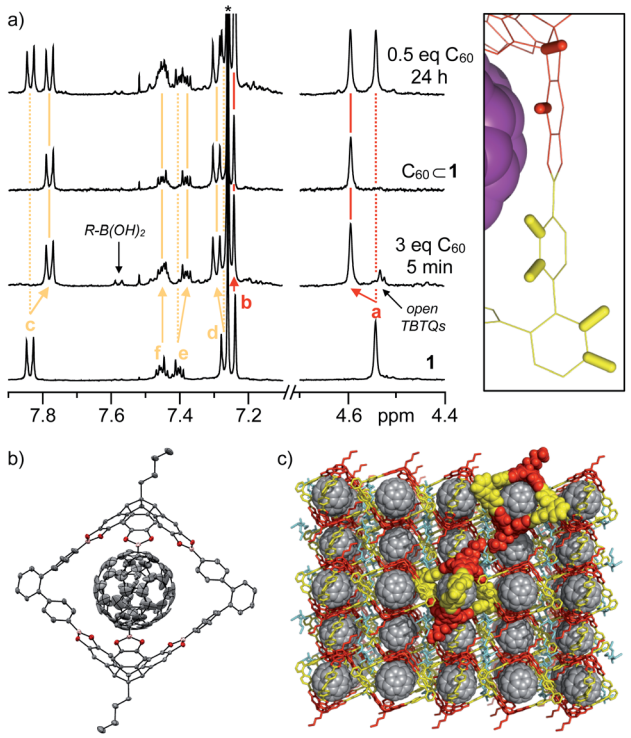

Fig. 3 (a) ^{1}H-NMR spectra (400 MHz, $CDCl_3$, rt) for complexation of **1** with C_{60}, (b) ORTEP representation of single-crystal X-ray structure of $C_{60}\subset$**1** (thermal ellipsoids were set at 50% probability, C = grey, O = red, B = purple, H atoms were omitted for clarity) and (c) packing of $C_{60}\subset$**1** in the solid state indicating the accessible C_{60} surface in the three cage windows.

and diamagnetic ring currents within the five- and six-membered rings of C_{60} are almost cancelling each other out. Directly after mixing, residual signals that can be attributed to free boronic acid and catechol moieties (Fig. 3a) suggest that encapsulation is achieved *via* partially opened cages and not *via* direct slipping. After one hour, cages **1** are again fully closed and quantitative complex formation is observed in case of equimolar mixtures or excess C_{60}. For substoichiometric fullerene concentrations, the appearance of two separate sets of signals for both **1** and $C_{60}\subset$**1** suggests a rather high kinetic stability for the assemblies, at least on the NMR time scale. For $C_{70}\subset$**1**, chemical shifts are more prominent, with the significant low-field shift for the aromatic TBTQ protons being particularly apparent (Fig. S2†). Therefore, we speculate that C_{70} is complexed in a more rigid fashion with the benzenoid hexagons of the equatorial belt being in close proximity to the axial TBTQ units and the fivefold rotational axes located along one of the cage windows. This model is also in accordance with semiempirical PM6 calculations (Fig. S1†). However, the exchange of the encapsulated C_{70} between the three windows should be fast, at least on the NMR time scale, as we did not observe any splitting of the signals for **1** in ^{1}H-NMR. In the ^{13}C-NMR spectrum of $C_{60}\subset$**1** (Fig. S3d†), a slight upfield shift from 143.24 to 141.65 ppm was observed for C_{60} upon complexation (Fig. S3e†). Due to the lower solubility of C_{70}, no ^{13}C-NMR spectrum could be measured in $CDCl_3$. For $C_{70}\subset$**1** however, five signals at 129.01, 143.72, 146.18, 146.63 and 149.63 ppm appeared, which are in very good agreement with values reported for C_{70} in C_6D_6 (130.28, 144.77, 146.82, 147.52, 150.07).[32]

Based on these analytical data, we concluded that the 1 : 1 complex $C_{60}\subset$**1** forms with very high thermodynamic and kinetic stability. A space filling model from the X-ray structure (Fig. 3c) further reveals that the aromatic scaffold of **1** shields a significant part of the C_{60} surface apart from the three cage windows arranged in a trigonal planar fashion. Therefore, we speculated on the potential of $C_{60}\subset$**1** acting as a supramolecular template for exohedral C_{60} functionalization. Assuming that each window can only accommodate one addend due to steric constraints, a limitation to trisaddition was anticipated. Furthermore, *trans*-3 and neighbouring addition patterns, which approach the 120° angle between two individual cage windows, should be favoured (Fig. 6 and S16†).

The Bingel[6] and Prato[7] reactions are the two most common methods for exohedral functionalization of fullerenes. For the twofold Bingel reaction, there is an intrinsic preference for *trans*-3 and *e*-addition,[13] whereas *cis*-addition is significantly disfavoured due to the steric demand of the ester substituents at the cyclopropane rings. For higher adducts, any pre-existing addends in *e*-position increasingly favour further *e*-addition, ultimately leading to the highly preferred T_h symmetrical hexakisaddition pattern.[33] Building upon this inherent selectivity, Ribas and coworkers reported on the exclusive formation of the all-equatorial tetrakisadduct for Bingel reactions on a complex of C_{60} within a tetragonal prismatic metallosupramolecular cage.[26] For the Prato reaction however, a much broader distribution of all eight possible bisadducts is usually observed (Fig. S12b†).[34] Only *trans*-1 and *cis*-1 isomers are formed in lower yields due to statistical (*t*1) and steric (*c*1) factors. Substantial *cis*-additions for smaller Prato addends generally result in very complex mixtures of higher adducts. In contrast to Bingel reactions, the isolation of specific regioisomers has only been reported in rare cases.[34a]

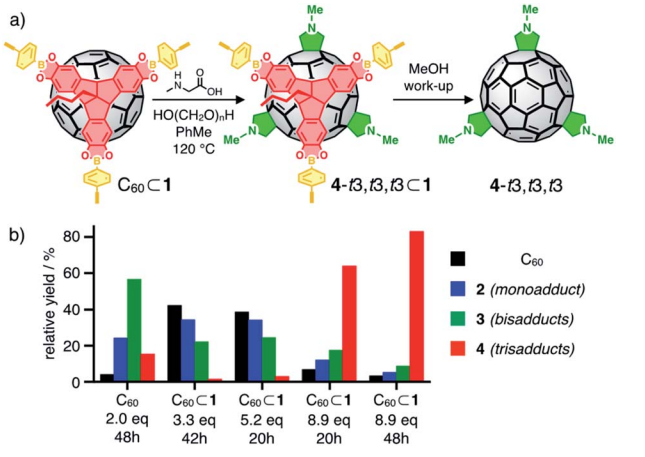

Fig. 4 (a) Cage-templated synthesis of *N*-methylfulleropyrrolidine trisadducts; (b) relative yields (based on HPLC integration) for unreacted C_{60} (black) and Prato adducts **2** (mono, blue), **3** (bis, green) and **4** (tris, red) for control experiment and cage-templated reactions.

Initial investigations for Bingel reactions on $C_{60}\subset\mathbf{1}$ gave promising hints for the selective formation of specific bis and trisadducts at the early stages. At higher conversion however, an increasing proportion of the undesired background reaction on free C_{60} was observed due to partial decomposition of the cages in the basic medium. Under Prato conditions though, cage **1** is sufficiently stable to restrict functionalization to the encapsulated C_{60}. As a model reaction, we chose the synthesis of *N*-methylfulleropyrrolidine multiple adducts $C_{60}(CH_2NCH_3CH_2)_n$ from sarcosine (Sar, *N*-methylglycine) and paraformaldehyde (Fig. 4a).

The use of formaldehyde as carbonyl component prevents the occurrence of complex mixtures of stereoisomers at the pyrrolidine rings. The implementation of Me as a very small *N*-substituent also ensures that any selectivity effect is primarily based on the inherent properties of the template and not on the steric demand of the addends. Ultimately, comprehensive data on HPLC elution profiles and spectroscopic signatures are available[34a,35] as reference for monoadduct **2** ($n = 1$), all regioisomeric bis (**3**, $n = 2$) and relevant trisadducts (**4**, $n = 3$).

To test the templating effect of cage **1**, varying equivalents of Sar and excess formaldehyde were added to solutions of $C_{60}\subset\mathbf{1}$ in 1 : 1 dry $CHCl_3$/toluene (or C_{60} in dry toluene as control) followed by heating under reflux (Fig. 4a, see ESI† for details) and reaction progress was monitored by MALDI-TOF MS. After specific time intervals, methanolic workup resulted in disassembly of the cages and the obtained fulleropyrrolidine mixtures were analyzed by analytical HPLC. As expected, multiple 1,3-dipolar cycloadditions on free C_{60} proceed rather unselective. After reaction with two equivalents Sar for eight hours, all eight regioisomeric bisadducts **3** and small amounts of trisadducts **4** were observed (Fig. 4b) in similar relative yields as previously reported (Fig. 5a and S12†).[34a] By contrast, reactions on $C_{60}\subset\mathbf{1}$ (Fig. 4b) proceed more slowly but with significantly higher selectivity. Reaction with up to 5 equivalents of Sar over 20 hours indicated low conversion with most of the C_{60} being unreacted (39% based on HPLC integration) or only converted to monoadduct **2** (34%). For the bisadducts **3** (24%), *cis*-addition is completely prevented and the symmetry-matched **3**-*t*3 is formed as the main regioisomer (Fig. 5b).

Intriguingly, even at low conversion significant amounts of D_3-symmetrical **4**-*t*3,*t*3,*t*3 (3%) are formed as the only detectable trisadduct. For this addition pattern, all three addends can be perfectly centred within the cage windows, thus minimizing any steric interactions between the addends and the cage walls.

By contrast, a control reaction on C_{60} with five equivalents of Sar for 20 hours resulted in a complex and inseparable mixture of many isomers with up to five pyrrolidine addends (Fig. S14a and d†). Reaction on $C_{60}\subset\mathbf{1}$ with 9 equivalents of Sar for 20 hours resulted in higher conversion and the predominant formation of trisadducts **4** (64%). According to MALDI-TOF MS for the reaction solution (Fig. S15a†), all fullerenes are still encapsulated and almost no higher adducts are formed. Remarkably, only four out of the possible 46 regioisomers for **4** were detected (Fig. 5c). Alongside the symmetry-matched **4**-*t*3,*t*3,*t*3 (25%) as the main product, only **4**-*t*4,*t*4,*t*2 (7%), **4**-*t*4,*t*3,*t*3 (8%) and **4**-*e*,*t*3,*t*2 (24% together with **3**-*e*) were observed as side products. This selectivity

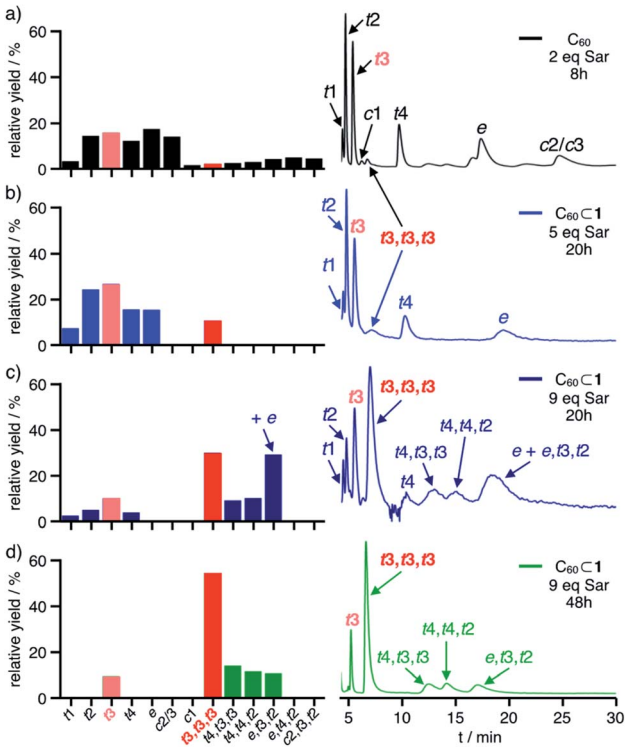

Fig. 5 Relative yields (left, calculated from HPLC profiles) for bisadducts **3** and trisadducts **4** and HPLC chromatograms (right) for (a) control experiment with C_{60} (2.0 eq. Sar, 8 h) and cage-templated reactions with $C_{60}\subset\mathbf{1}$ and (b) 5 eq. Sar (20 h), (c) 9 eq. Sar (20 h) and (d) 9 eq. Sar (48 h, preparative scale); yields for **3**-*t*3 and **4**-*t*3,*t*3,*t*3 are indicated in light red and red, respectively.

can be nicely explained by molecular models for the *trans*- and *e*-bisadduct complexes $\mathbf{3}\subset\mathbf{1}$ (see Fig. S17†), since any addition to double bonds centred in the third window leads exclusively to these four isomers (Fig. 6). Cage **1** acts as a supramolecular shadow mask that prevents over-functionalization and templates the addition in *trans*-3 and related positions. Indeed, no *cis*-adducts and only those four trisadducts, which best match the trigonal planar arrangement of the cage windows, were observed throughout the reaction time (Fig. 5).

For the non-templated reaction,[34a] nine different trisadducts **4** have been isolated in a combined yield of 4.4% (Fig. S24†) only after tedious chromatographic separation that involved several preparative TLC and HPLC steps. Thereby, **4**-*t*3,*t*3,*t*3 was obtained as the minor isomer in only 0.2% yield. When running the cage-templated reaction (Fig. 4a) on a preparative scale, it proved advantageous to add up to 9 equivalents of Sar in three batches and to extend reaction times to 48 hours (see ESI† for details). For these prolonged reactions, the emerging decomposition of cage **1** initiated some overreaction outside of the cages (see Fig. S19a† for MALDI-TOF MS). Apparently, all mismatched isomers react faster, thus further simplifying the remaining mixture and increasing the relative yield for the matching **3**-*t*3 and **4**-*t*3,*t*3,*t*3 (Fig. 5d).

After methanolic work-up, all five remaining bis and trisadducts could be purified by one single automated flash chromatography run without the need for tedious HPLC

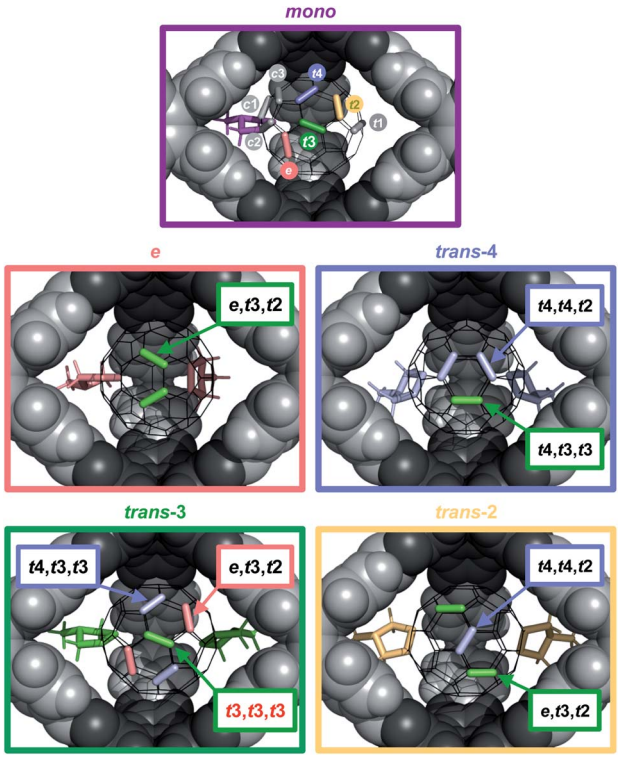

Fig. 6 Accessibility of specific addition patterns in the cage windows for a second addition on **2**⊂**1** (top, first addend purple) and a third addition on **3**-*e*⊂**1** (middle left, *e*-addends in red), **3**-*t*4⊂**1** (middle right, *t*4-addends in blue), **3**-*t*3⊂**1** (bottom left, *t*3-addends in green) and **3**-*t*2⊂**1** (bottom right, *t*2-addends in yellow).

separation. Finally, the four different trisadducts were isolated as pure regioisomers in a one-pot-reaction starting from pristine C_{60} with a combined yield of 16%. All products were analyzed by MALDI-TOF MS (Fig. S22†) and comparison of UV/Vis (Fig. S23†) and ^{1}H-NMR spectra (Fig. S20 and S21†) to literature data.[34a] When compared to the rather nonselective control reaction, the selectivity for the cage-templated reaction is completely reversed and the isolated yield for **4**-*t*3,*t*3,*t*3 as the main product is increased by a factor of 30 (Fig. S24†). The small pore windows of **1** enforce the formation of the unfavoured *t*3,*t*3,*t*3-addition pattern that would otherwise only be obtained in trace amounts. On the other hand, the cage walls prevent overreaction to higher adducts. In future work, we plan to optimize reaction conditions for a further increase in isolated amounts of pure trisadducts, modify the cage windows to enhance the selectivity and develop more stable cages to perform more sensitive reactions.

Conclusions

In summary, we have demonstrated the efficient fullerene encapsulation within the pores of trigonal bipyramidal covalent organic cage **1**. Due to suitable preorganization of its two TBTQ moieties, strong 1 : 1 complexes C_{60}⊂**1** and C_{70}⊂**1** are formed in organic solvents and binding constants of $6.3 \pm 0.4 \times 10^5$ and $5.3 \pm 0.4 \times 10^5$ M^{-1}, respectively, have been determined by UV/Vis titrations. As evidenced by an X-ray structure for C_{60}⊂**1**, only three distinct parts of the C_{60} surface are accessible for exohedral functionalization. In prototypical Prato reactions on C_{60}⊂**1**, remarkable selectivity for the symmetry-matched trisadduct **4**-*t*3,*t*3,*t*3, which is formed only in trace amounts in cage-free reactions, was observed. Cage **1** acts as an efficient supramolecular shadow mask, whose small pore windows force the formation of an otherwise unfavoured trisaddition pattern. These exciting findings are the first example for a supramolecular control of the regioselectivity for the intrinsically nonselective Prato reaction. They will pave the way for novel applications of covalent organic cage compounds as effective templates for spatially precise reactions on large spherical π-systems.

Conflicts of interest

There are no conflicts to declare.

Acknowledgements

This work was financially supported by the Fonds der Chemischen Industrie (Liebig fellowship for FB and doctoral fellowship for SF), the DFG (BE4808/2-1) and the Collaborative Research Network "Solar Technologies Go Hybrid" of the Bavarian Ministry of Science, Research and the Arts.

Notes and references

1 R. Taylor and D. R. M. Walton, *Nature*, 1993, **363**, 685–693.
2 (*a*) E. Castro, A. H. Garcia, G. Zavala and L. Echegoyen, *J. Mater. Chem. B*, 2017, **5**, 6523–6535; (*b*) F. Beuerle, R. Lebovitz and A. Hirsch, in *Medicinal Chemistry and Pharmacological Potential of Fullerenes and Carbon Nanotubes*, 2008, vol. 1, pp. 51–78.
3 (*a*) C.-Z. Li, H.-L. Yip and A. K.-Y. Jen, *J. Mater. Chem.*, 2012, **22**, 4161–4177; (*b*) G. Dennler, M. C. Scharber and C. J. Brabec, *Adv. Mater.*, 2009, **21**, 1323–1338.
4 D. M. Guldi, B. M. Illescas, C. M. Atienza, M. Wielopolski and N. Martin, *Chem. Soc. Rev.*, 2009, **38**, 1587–1597.
5 M. Tsuda, T. Ishida, T. Nogami, S. Kurono and M. Ohashi, *Chem. Commun.*, 1993, 1296–1298.
6 C. Bingel, *Chem. Ber.*, 1993, **126**, 1957–1959.
7 M. Maggini, G. Scorrano and M. Prato, *J. Am. Chem. Soc.*, 1993, **115**, 9798–9799.
8 W. Zhang and T. M. Swager, *J. Am. Chem. Soc.*, 2007, **129**, 7714–7715.
9 (*a*) A. Hirsch and M. Brettreich, *Fullerenes — Chemistry and Reactions*, Wiley-VCH, Weinheim, 2005; (*b*) C. Thilgen and F. Diederich, *Chem. Rev.*, 2006, **106**, 5049–5135; (*c*) W. Yan, S. M. Seifermann, P. Pierrat and S. Bräse, *Org. Biomol. Chem.*, 2015, **13**, 25–54; (*d*) A. Hirsch, I. Lamparth and H. R. Karfunkel, *Angew. Chem., Int. Ed.*, 1994, **33**, 437–438; (*e*) F. Djojo, A. Hirsch and S. Grimme, *Eur. J. Org. Chem.*, 1999, 3027–3039.
10 (*a*) F. Hörmann and A. Hirsch, *Chem.–Eur. J.*, 2013, **19**, 3188–3197; (*b*) S. K. Dey, F. Beuerle, M. A. Olson and J. F. Stoddart,

Chem. Commun., 2011, **47**, 1425–1427; (*c*) A. Muñoz, D. Sigwalt, B. M. Illescas, J. Luczkowiak, L. Rodríguez-Pérez, I. Nierengarten, M. Holler, J.-S. Remy, K. Buffet, S. P. Vincent, J. Rojo, R. Delgado, J.-F. Nierengarten and N. Martín, *Nat. Chem.*, 2016, **8**, 50–57; (*d*) S. Guerra, J. Iehl, M. Holler, M. Peterca, D. A. Wilson, B. E. Partridge, S. Zhang, R. Deschenaux, J.-F. Nierengarten and V. Percec, *Chem. Sci.*, 2015, **6**, 3393–3401; (*e*) B. M. Illescas, J. Rojo, R. Delgado and N. Martín, *J. Am. Chem. Soc.*, 2017, **139**, 6018–6025; (*f*) M. Riala, K. L. Maxouti, C. P. Ioannou and N. Chronakis, *Org. Lett.*, 2016, **18**, 1132–1135; (*g*) F. Beuerle and A. Hirsch, *Chem.–Eur. J.*, 2009, **15**, 7447–7455.

11 (*a*) A. Kraft and F. Beuerle, *Tetrahedron Lett.*, 2016, **57**, 4651–4663; (*b*) A. M. Rice, E. A. Dolgopolova and N. B. Shustova, *Chem. Mater.*, 2017, **29**, 7054–7061; (*c*) A. L. Balch and K. Winkler, *Chem. Rev.*, 2016, **116**, 3812–3882; (*d*) P. Peng, F.-F. Li, V. S. P. K. Neti, A. J. Metta-Magana and L. Echegoyen, *Angew. Chem., Int. Ed.*, 2014, **53**, 160–163; (*e*) A. Kraft, P. Roth, D. Schmidt, J. Stangl, K. Müller-Buschbaum and F. Beuerle, *Chem.–Eur. J.*, 2016, **22**, 5982–5987; (*f*) A. Kraft, C. Roger, D. Schmidt, J. Stangl, K. Müller-Buschbaum and F. Beuerle, *Chem.–Eur. J.*, 2017, **23**, 15864–15868.

12 (*a*) A. Kraft, M. Gsänger and F. Beuerle, *Eur. J. Org. Chem.*, 2014, 523–528; (*b*) A. Kraft, J. Stangl, A.-M. Krause, K. Müller-Buschbaum and F. Beuerle, *Beilstein J. Org. Chem.*, 2017, **13**, 1–9; (*c*) E. Fernandez-Bartolome, J. Santos, A. Gamonal, S. Khodabakhshi, L. J. McCormick, S. J. Teat, E. C. Sañudo, J. S. Costa and N. Martín, *Angew. Chem., Int. Ed.*, 2019, **58**, 2310–2315.

13 F. Djojo, A. Herzog, I. Lamparth, F. Hampel and A. Hirsch, *Chem.–Eur. J.*, 1996, **2**, 1537–1547.

14 P. R. Birkett, A. G. Avent, A. D. Darwish, H. W. Kroto, R. Taylor and D. R. M. Walton, *J. Chem. Soc., Chem. Commun.*, 1993, 1230–1232.

15 M. Sawamura, H. Iikura and E. Nakamura, *J. Am. Chem. Soc.*, 1996, **118**, 12850–12851.

16 (*a*) I. Lamparth, C. Maichle-Mössmer and A. Hirsch, *Angew. Chem., Int. Ed.*, 1995, **34**, 1607–1609; (*b*) A. Hirsch and O. Vostrowsky, *Eur. J. Org. Chem.*, 2001, **2001**, 829–848.

17 L. Isaacs, R. F. Haldimann and F. Diederich, *Angew. Chem., Int. Ed.*, 1994, **33**, 2339–2342.

18 (*a*) U. Reuther, T. Brandmüller, W. Donaubauer, F. Hampel and A. Hirsch, *Chem.–Eur. J.*, 2002, **8**, 2261–2273; (*b*) F. Beuerle, N. Chronakis and A. Hirsch, *Chem. Commun.*, 2005, 3676–3678; (*c*) F. Beuerle and A. Hirsch, *Chem.–Eur. J.*, 2009, **15**, 7434–7446.

19 G. Bottari, O. Trukhina, A. Kahnt, M. Frunzi, Y. Murata, A. Rodríguez-Fortea, J. M. Poblet, D. M. Guldi and T. Torres, *Angew. Chem., Int. Ed.*, 2016, **55**, 11020–11025.

20 Y. Xu, R. Kaur, B. Wang, M. B. Minameyer, S. Gsanger, B. Meyer, T. Drewello, D. M. Guldi and M. von Delius, *J. Am. Chem. Soc.*, 2018, **140**, 13413–13420.

21 (*a*) T. Kawase and H. Kurata, *Chem. Rev.*, 2006, **106**, 5250–5273; (*b*) K. Tashiro and T. Aida, *Chem. Soc. Rev.*, 2007, **36**, 189–197; (*c*) C. García-Simón, M. Costas and X. Ribas, *Chem. Soc. Rev.*, 2016, **45**, 40–62; (*d*) C. Yu, Y. Jin and W. Zhang, *Chem. Rec.*, 2015, **15**, 97–106; (*e*) D. Canevet, E. M. Pérez and N. Martín, *Angew. Chem., Int. Ed.*, 2011, **50**, 9248–9259; (*f*) F. Beuerle and B. Gole, *Angew. Chem., Int. Ed.*, 2018, **57**, 4850–4878; (*g*) C. García-Simón, A. Monferrer, M. Garcia-Borràs, I. Imaz, D. Maspoch, M. Costas and X. Ribas, *Chem. Commun.*, 2019, **55**, 798–801; (*h*) V. Martínez-Agramunt, T. Eder, H. Darmandeh, G. Guisado-Barrios and E. Peris, *Angew. Chem., Int. Ed.*, 2019, **58**, 5682–5686.

22 (*a*) C. Zhang, Q. Wang, H. Long and W. Zhang, *J. Am. Chem. Soc.*, 2011, **133**, 20995–21001; (*b*) C. Fuertes-Espinosa, A. Gómez-Torres, R. Morales-Martínez, A. Rodríguez-Fortea, C. García-Simón, F. Gándara, I. Imaz, J. Juanhuix, D. Maspoch, J. M. Poblet, L. Echegoyen and X. Ribas, *Angew. Chem., Int. Ed.*, 2018, **57**, 11294–11299; (*c*) M.-J. Li, C.-H. Huang, C.-C. Lai and S.-H. Chiu, *Org. Lett.*, 2012, **14**, 6146–6149; (*d*) W. Sun, Y. Wang, L. Ma, L. Zheng, W. Fang, X. Chen and H. Jiang, *J. Org. Chem.*, 2018, **83**, 14667–14675.

23 (*a*) Y. Xu, B. Wang, R. Kaur, M. B. Minameyer, M. Bothe, T. Drewello, D. M. Guldi and M. von Delius, *Angew. Chem., Int. Ed.*, 2018, **57**, 11549–11553; (*b*) M. Ortiz, S. Cho, J. Niklas, S. Kim, O. G. Poluektov, W. Zhang, G. Rumbles and J. Park, *J. Am. Chem. Soc.*, 2017, **139**, 4286–4289; (*c*) S. Bähring, K. R. Larsen, M. Supur, K. A. Nielsen, T. Poulsen, K. Ohkubo, C. W. Marlatt, E. Miyazaki, K. Takimiya, A. H. Flood, S. Fukuzumi and J. O. Jeppesen, *Chem. Commun.*, 2017, **53**, 9898–9901; (*d*) J. Rio, S. Beeck, G. Rotas, S. Ahles, D. Jacquemin, N. Tagmatarchis, C. Ewels and H. A. Wegner, *Angew. Chem., Int. Ed.*, 2018, **57**, 6930–6934.

24 W. Brenner, T. K. Ronson and J. R. Nitschke, *J. Am. Chem. Soc.*, 2017, **139**, 75–78.

25 B. Chen, J. J. Holstein, S. Horiuchi, W. G. Hiller and G. H. Clever, *J. Am. Chem. Soc.*, 2019, **141**, 8907–8913.

26 C. Fuertes-Espinosa, C. García-Simón, M. Pujals, M. Garcia-Borràs, L. Gómez, T. Parella, J. Juanhuix, I. Imaz, D. Maspoch, M. Costas and X. Ribas, *Chem*, 2020, **6**, 169–186.

27 R. Schwenninger, T. Müller and B. Kräutler, *J. Am. Chem. Soc.*, 1997, **119**, 9317–9318.

28 (*a*) D. Kuck, *Angew. Chem., Int. Ed.*, 1984, **23**, 508–509; (*b*) D. Kuck, *Chem. Rev.*, 2006, **106**, 4885–4925; (*c*) A. Dhara and F. Beuerle, *Synthesis*, 2018, **50**, 2867–2877.

29 (*a*) G. Zhang and M. Mastalerz, *Chem. Soc. Rev.*, 2014, **43**, 1934–1947; (*b*) T. Hasell and A. I. Cooper, *Nat. Rev. Mater.*, 2016, **1**, 16053; (*c*) M. Mastalerz, *Acc. Chem. Res.*, 2018, **51**, 2411–2422.

30 (*a*) S. Klotzbach, T. Scherpf and F. Beuerle, *Chem. Commun.*, 2014, **50**, 12454–12457; (*b*) S. Klotzbach and F. Beuerle, *Angew. Chem., Int. Ed.*, 2015, **54**, 10356–10360.

31 (*a*) B. Bredenkötter, S. Henne and D. Volkmer, *Chem.–Eur. J.*, 2007, **13**, 9931–9938; (*b*) S. Henne, B. Bredenkötter, A. A. Dehghan Baghi, R. Schmid and D. Volkmer, *Dalton Trans.*, 2012, **41**, 5995–6002; (*c*) B. Bredenkötter, M. Grzywa, M. Alaghemandi, R. Schmid, W. Herrebout, P. Bultinck and D. Volkmer, *Chem.–Eur. J.*, 2014, **20**, 9100–9110; (*d*) S. Henne, B. Bredenkötter, M. Alaghemandi, S. Bureekaew, R. Schmid and D. Volkmer, *ChemPhysChem*,

2014, **15**, 3855–3863; (*e*) T. Wang, Z.-Y. Li, A.-L. Xie, X.-J. Yao, X.-P. Cao and D. Kuck, *J. Org. Chem.*, 2011, **76**, 3231–3238; (*f*) P. E. Georghiou, L. N. Dawe, H.-A. Tran, J. Strübe, B. Neumann, H.-G. Stammler and D. Kuck, *J. Org. Chem.*, 2008, **73**, 9040–9047.

32 R. Taylor, J. P. Hare, A. K. Abdul-Sada and H. W. Kroto, *Chem. Commun.*, 1990, 1423–1425.

33 A. Hirsch, I. Lamparth, T. Grösser and H. R. Karfunkel, *J. Am. Chem. Soc.*, 1994, **116**, 9385–9386.

34 (*a*) S. Marchesan, T. Da Ros and M. Prato, *J. Org. Chem.*, 2005, **70**, 4706–4713; (*b*) Q. Lu, D. I. Schuster and S. R. Wilson, *J. Org. Chem.*, 1996, **61**, 4764–4768.

35 T. Nishimura, K. Tsuchiya, S. Ohsawa, K. Maeda, E. Yashima, Y. Nakamura and J. Nishimura, *J. Am. Chem. Soc.*, 2004, **126**, 11711–11717.